

# QUADRUPED OPTIMUM GAITS ANALYSIS FOR PLANETARY EXPLORATION

Ioannis Kontolatis <sup>(1)</sup>, Dimitrios Myrasiotis <sup>(1)</sup>, Iosif Paraskevas <sup>(1)</sup>,  
Evangelos Papadopoulos <sup>(1)</sup>, Guido de Croon <sup>(2)</sup>, Dario Izzo <sup>(2)</sup>

<sup>(1)</sup>Control Systems Laboratory, Department of Mechanical Engineering, National Technical University of Athens,  
9, Heroon Polytechniou Str., 15780 Zografou, Athens, Greece

Email: ikontol@central.ntua.gr, dimyrisiotis@gmail.com, isparas@mail.ntua.gr, egpapado@central.ntua.gr

<sup>(2)</sup>Advanced Concepts Team, European Space Agency,  
PPC-PF, ESTEC, Keplerlaan 1, 2201 AZ Noordwijk, The Netherlands  
Email: guido.de.croon@esa.int, dario.izzo@esa.int

## ABSTRACT

Leg compliance, gravity and ground have a significant impact on the performance and gait characteristics of a quadruped robot. This paper presents results obtained using a planar lumped parameter model of a quadruped robot and an extensive research scheme to determine optimum design parameters for a quadruped moving in different gravity environments. Hildebrand diagrams are used to classify quadruped robot gaits. In addition, an optimization procedure using either MathWorks *fmincon* or a Differential Evolutionary (DE) algorithm is employed to determine the optimum motion and robot physical parameters related to energy efficiency. Using “multiple gait graphs”, the effects of leg compliance, gravity and ground inclination are determined.

## 1. INTRODUCTION

Legged locomotion offers a great potential to mobile platforms transversing unstructured environments in terms of speed, energy efficiency and adaptation. Planets, satellites, and asteroids presenting great scientific and exploration interest, are all characterized by such environments and therefore are candidates for legged robot deployment. Research in legged locomotion led to several models, control algorithms and designs.

To name a few, researchers at the JPL proposed the ATHLETE concept, a six-limbed hybrid mobile platform designed to traverse terrain using its wheels or limbs [1]. Another six-legged robot proposed for planetary exploration is the DLR Crawler [2], an actively compliant walking robot that implements a walking layer with a simple tripod and a more complex biologically inspired gait. The robot ASTRO, part of an emulation testbed for asteroid exploration, is a six-limbed ambulatory locomotion system that replicates walking gaits of the arachnid insects [3]. DFKI researchers presented SpaceClimber, a biologically inspired six-legged robot for steep slopes, and focused on the foot-design to handle constraints from the environmental ground conditions [4]. Researchers from ASL/ ETH proposed a quadruped that was built for upright walking but its wide range of motion in all joints

allows a crawling gait and recovery manoeuvres [5]. However, these robots perform statically stable gaits for the sake of overall motion stability and rough terrain handling, which reduces their speed capability.

In addition, a general systematic approach to the design and selection of optimal robot gaits is lacking. The way that quadruped animals walk has been studied intensively since 1887 [6] and many results that refer to connections between their walking nature and their body and structure characteristics have been presented [7]. Also, systematical ways to observe and classify their moving behaviour have been developed. Hildebrand adopted graphical ways, which present the back and front legs duty factors as well as the phase difference between the legs of the same side (left or right) as a percentage of the stride duration, i.e. the time interval between two successive footfalls (touchdowns) of the back left foot [8]. These definitions are implemented in practical experiments [9], [10].

In this paper, we focus in the systematic use of Hildebrand diagrams in analyzing quadruped robot gaits that result from an extensive search process. Environmental conditions taken into consideration include gravity, topographic features, surface and subsurface characteristics. A point contact/impact between foot and surface is assumed.

An optimization procedure using either MathWorks *fmincon* or a Differential Evolutionary (DE) optimization algorithm is employed to determine the optimum motion initial conditions, quadruped model physical parameters and the desired motion parameters related to energy efficiency.

The resulting gaits are classified using an automated scheme based on the Hildebrand gait diagram and gait graph. Using multiple gait graphs, a general plot for a significant parameter is formed which depicts on the same plane the gait graphs of a number of simulations that differ by one parameter each time, e.g. leg stiffness. Resulting “multiple gait graphs” show that gravity increase leads to the increase of the mean value of the Duty Factor, ground inclination increase leads to the increase of the Phase Relationship value and leg stiffness increase leads to the decrease of the mean value of the Duty Factor.

## 2. SYSTEM DYNAMICS

### 2.1. Robot Model

Fig. 1 shows a lumped parameter physical model of the quadruped robot employed in this paper. The model consists of two compliant virtual legs (VLegs) of mass  $m_j$  and uncompressed length  $l_{0j}$ , and a body of mass  $m_b$  and inertia  $I_b$  respectively. The index  $j$  indicates a rear ( $r$ ) or a front ( $f$ ) VLeg. A VLeg, front or rear, models the two respective physical legs that operate in pairs when a gait is realized and exerts equal torques and forces on the body as the set of the two physical ones [11].

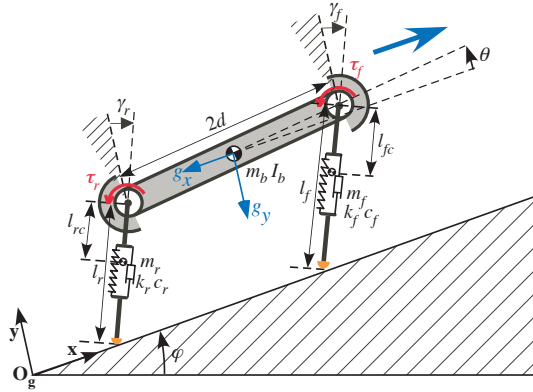


Figure 1. A lumped parameter planar quadruped model.

Each VLeg is connected to the main body with an actuated rotational joint at distance  $d$  from the body center of mass (CM). This body can rotate by an angle  $\theta$  around the  $z$ -axis and thus the model captures the body pitch stabilization problem. The rotational hip joint allows for positioning of VLegs at angle  $\gamma_j$  in the sagittal plane. Also, each VLeg has a passive prismatic joint modeled as a linear compression spring of constant  $k_j$  and viscous damping coefficient  $c_j$ . The prismatic joint allows changes of the VLeg length  $l_j$  and energy accumulation during locomotion. Table 1 summarizes robot and motion parameters.

Table 1. Nomenclature.

Symbol	Quantity
$x_c$	Body CM x-axis coordinate
$y_c$	Body CM y-axis coordinate
$\theta$	Body pitch angle
$I_b$	Body inertia w.r.t. z-axis
$m_b$	Body mass
$x$	VLeg CM x-axis coordinate
$y$	VLeg CM y-axis coordinate
$l$	VLeg length
$l_0$	VLeg uncompressed length
$k$	VLeg spring constant
$c$	VLeg viscous dumping coefficient
$\gamma$	VLeg absolute angle
$I_l$	VLeg inertia w.r.t. z-axis
$m$	VLeg mass

$d$	Hip joint to CM distance
$\phi$	Ground inclination
$\tau$	Hip torque
$r$	As index: rear VLeg
$f$	As index: front VLeg
$td$	As index: value at touchdown
$lo$	As index: value at liftoff

### 2.2. Motion Phases and Transitions

A quadruped robot, studied in the sagittal plane, goes through four phases of the three-link (rear VLeg, front VLeg, main body) kinematic chain, i.e. double stance, flight, front stance, rear stance, as presented in Fig. 2. The realization of the gait depends on which legs are working in pairs, which motion phases appear and for how long, the values of the leg touchdown angles and body pitch angle.

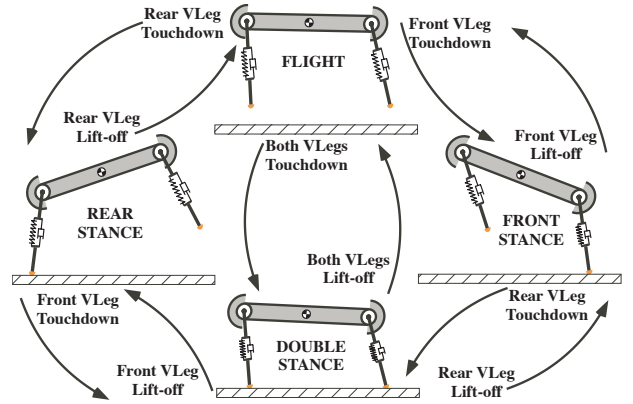


Figure 2. Motion phases and events that trigger them.

Pronking is the gait when all legs are, either in contact with the ground (double stance) or not (flight). The bounding gait has two additional intermediate phases, namely the ones in which only one set of legs (rear or front) is in contact with the ground. In pronking, zero or close to zero pitching is expected. However, in the non-ideal case, where body pitching occurs, the rear or front legs may strike the ground first. Then, pronking reduces to bounding.

Legged robots are hybrid systems and therefore their motion cannot be described by a single set of equations. A set of continuous equations for each phase together with discrete transformations governing transitions from one phase to the next are required to model the dynamics of such systems. The transition equations that determine the touchdown and lift-off events of the rear and front VLegs during plane motion are:

$$y_c - d \sin(\theta_{td}) \leq l_{0r} \cos(\gamma_{r,td}) \quad (1)$$

$$y_c + d \sin(\theta_{td}) \leq l_{0f} \cos(\gamma_{f,td}) \quad (2)$$

$$l_{r,lo} = l_{0r} \quad (3)$$

$$l_{f,lo} = l_{0f} \quad (4)$$

Eqs. (1) and (2) describe the conditions of touchdown events, while (3) and (4) describe the conditions of

liftoff events. Which event will occur depends on length comparison.

### 2.3. Equations of Motion

The robot motion is studied in the sagittal plane. During the flight phase (both VLegs do not touch the ground), the robot's CM performs a ballistic motion with constant system angular momentum with respect to the CM. During stance phase, the VLeg(s) that are in contact with the ground move the body forward. The equations of motion for the main phases, i.e. flight (*FL*) and double stance (*ST*), and for the intermediate ones, i.e. front (*FST*) and rear stance (*RST*), are derived using a Lagrangian formulation. During double stance phase the vector of the generalized coordinates is

$$\mathbf{q}_{ST} = \begin{bmatrix} x_c & y_c & \theta & \gamma_r & \gamma_f \end{bmatrix}^T \quad (5)$$

and the Lagrangian of the robot is:

$$\begin{aligned} L_{RobotST} &= L_{BodyST} + L_{VLegST} + L_{VLegFST} = \\ &\frac{1}{2}m_b(\dot{x}_c^2 + \dot{y}_c^2) + \frac{1}{2}I_b\dot{\theta}^2 - m_b g_x x_c - m_b g_y y_c \\ &+ \frac{1}{2}m_r(\dot{x}_r^2 + \dot{y}_r^2) - \frac{1}{2}k_r(l_{0r} - l_r)^2 - m_r g_x x_r - m_r g_y y_r \\ &+ \frac{1}{2}m_f(\dot{x}_f^2 + \dot{y}_f^2) - \frac{1}{2}k_f(l_{0f} - l_f)^2 - m_f g_x x_f - m_f g_y y_f \end{aligned} \quad (6)$$

The ground inclination, positive or negative, affects robot dynamics through the two gravity components  $g_x$ ,  $g_y$ :

$$g_x = g \cdot \sin(\varphi), \quad g_y = g \cdot \cos(\varphi) \quad (7)$$

Rear ( $x_r, y_r$ ) and front ( $x_f, y_f$ ) VLeg CM coordinates can be expressed as functions of the generalized coordinates using geometrical relationships:

$$x_r = x_c - d \cos(\theta) + l_{rc} \sin(\gamma_r) \quad (8)$$

$$y_r = y_c - d \sin(\theta) - l_{rc} \cos(\gamma_r)$$

$$x_f = x_c + d \cos(\theta) + l_{fc} \sin(\gamma_f) \quad (9)$$

$$y_f = y_c + d \sin(\theta) - l_{fc} \cos(\gamma_f)$$

The energy dissipation due to prismatic joint viscous damping is:

$$P_{Diss} = \frac{1}{2}c_r \dot{l}_r^2 + \frac{1}{2}c_f \dot{l}_f^2 \quad (10)$$

The energy contribution of actuator torques is given by:

$$P_{Contr} = \tau_r (\dot{\gamma}_r - \dot{\theta}) + \tau_f (\dot{\gamma}_f - \dot{\theta}) \quad (11)$$

Variables  $l_r$ ,  $\gamma_r$ ,  $l_f$ ,  $\gamma_f$  are derived using kinematic relationships:

$$l_r = \sqrt{(x_{tr,td} + d \cos(\theta) - x_c)^2 + (d \sin(\theta) - y_c)^2} \quad (12)$$

$$\gamma_r = \text{Arctan}(-d \sin(\theta) + y_c, x_{tr,td} + d \cos(\theta) - x_c) \quad (13)$$

$$l_f = \sqrt{(x_{tf,td} - d \cos(\theta) - x_c)^2 + (d \sin(\theta) - y_c)^2} \quad (14)$$

$$\gamma_f = \text{Arctan}(d \sin(\theta) + y_c, x_{tf,td} - d \cos(\theta) - x_c) \quad (15)$$

Rear  $x_{tr,td}$  and front  $x_{tf,td}$  toe location are given by:

$$x_{tr,td} = x_c + l_r \sin(\gamma_r) - d \cos(\theta) \quad (16)$$

$$x_{tf,td} = x_c + l_f \sin(\gamma_f) + d \cos(\theta) \quad (17)$$

when touchdown occurs without toe slippage.

During the flight phase the generalized coordinates vector is the same as (5) and the Lagrangian of the robot is (6) with the spring terms omitted, while there is no energy dissipation and contribution. For the two intermediate phases, i.e. rear and front stance, vector  $\mathbf{q}_i$  does not include  $l_r$ ,  $\gamma_r$  or  $l_f$ ,  $\gamma_f$  respectively, which are calculated again by (12), (13) and (14), (15), and the Lagrangian, energy dissipation and contribution equations of each phase miss the appropriate terms. Equations of motion for all phases are derived as:

$$\frac{d}{dt} \left( \frac{\partial L_{Robot i}}{\partial \dot{\mathbf{q}}_i} \right) - \left( \frac{\partial L_{Robot i}}{\partial \mathbf{q}_i} \right) + \left( \frac{\partial P_{Diss i}}{\partial \dot{\mathbf{q}}_i} \right) - \left( \frac{\partial P_{Contr i}}{\partial \dot{\mathbf{q}}_i} \right) = \mathbf{0} \quad (18)$$

where  $i$  is the phase index, i.e. *ST*, *FL*, *RST*, *FST*.

### 3. GROUND MODELS

The environmental conditions affect the motion of a legged system therefore it is necessary to develop models that shall quantify their relation with the emerged gaits. The environmental parameters that have direct effect on motion types are: gravity, topographic features, surface and subsurface characteristics. Other parameters which have indirect effect but can be modelled sufficiently by changing the characteristics of the body and legs are: environmental radiation, temperature, pressure, corrosive environment and weather of celestial body. For example in the case of environmental radiation a larger mass would correspond to the inclusion of a radiation protection system. To this end, this analysis will focus on the first four parameters, which are the most crucial and cannot be modelled via an indirect way without loss of realism. Particular attention will be given to the subsurface characteristics.

#### 3.1. Gravity

This parameter plays a dominant role during the definition of the best strategy for gaits, as it was evident by the astronauts' movements on the Moon. Gravity has direct implication on the motion the robot. At the limit of zero gravity, no gait of any kind is possible. Additionally, gravity defines the apex height of the gait, e.g. a large stride at a planet with low gravity may result the landing of the robot far from a scientific goal of interest. Whilst gravity has a dominant role, the modelling of gravity is rather simple. The dynamic model of the robot system explicitly includes the gravitational acceleration which is defined by references like [12].

#### 3.2. Topographic Features

The surface of celestial bodies is not flat and the slope on any area of interest is expected to be variational. Of great scientific importance are craters or similar features (e.g. mountain or volcanoes), and the inclination on

these areas imposes various dangers for any robot (e.g. tipping over), especially when a dynamically stable gait is used. It is necessary to model the inclinations in such a way that safe results could be obtained. Each path of the robot is separated in small segments with local inclinations (defined by the global inclination characteristics). The user defines only the dimensions of these segments, length for the 2D case, length and width for the 3D case. Note that all the properties of the terrain at a point are defined by the properties of the segment they belong.

### 3.3. Surface Characteristics

The coverage of an area from rocks or soil, affect the path profile of the robot. The rock dimensions are directly related to the gait that the robot should use to pass over without tipping. Moreover when touchdown occurs, it is highly possible the legs to be in different levels due to uneven terrain characteristics, such as different rock sizes. Various distribution models can be applied for this reason, for example for Mars, distribution model equations can be found in [13]. On the simulation, the existence of rocks can be modelled by changing locally and abruptly the local inclination.

### 3.4. Subsurface Characteristics

The terrain includes areas with regolith and bedrocks that can be comprised of materials with different properties [14]. Similar information can be obtained for other planets, satellites or asteroids. In addition, the compliance of the ground affects the motion and different contact models and/or parameters should be applied according to the nature of the terrain, e.g. granular soil could be implemented as a surface with large deformations, and a rocky surface as a fixed body with large stiffness. Stick, slip and sliding conditions should be taken into account, with surface friction playing dominant role [15].

Since space agencies have shown in the past large interest on rover locomotion, various terramechanics models have been developed or exemplified for the case of planets, such as in [16]. Related work on the past took place for the case of legged locomotion with combined use of artificial intelligence schemes for real time estimation of soil parameters [17]. These works have as a common feature the use of equations that make use Bekker equations or similar. However, as [18] also presents, this approach lacks on the accurate representation of a dynamics interaction between soils and legs – and for this reason the authors introduce the term “terradyamics”. This approach is proved interesting for the locomotion of the robot types that the authors examine but does not include impact characteristics, which are prominent in our case. However the term terradyamics can be equally used in our approach.

Generally impacts can be modelled via three

methods, which are presented in [19]. The use of compliant models seems the most appropriate, as the different soil kinds can be simulated by lumped parameters (i.e. springs and dampers) with different linear or non-linear characteristics. The simulation exploits the properties of springs and dampers in series. That is, the spring and/ or damper of the leg and terrain are in series and an equivalent stiffness and/ or damper is used. As a first approach this can lead to some simplifications (e.g. if a very stiff ground exists, then leg stiffness dominates).

Currently there is work in progress for implementation of more detailed ground models using viscoelastic models like Kelvin – Voigt

$$F = K \cdot x + B \cdot \dot{x} \quad (19)$$

and Hunt – Crossley

$$F = K \cdot x^n + B \cdot \dot{x} \cdot x^n \quad (20)$$

where  $K, B$  are the stiffness and damping coefficients,  $n$  a parameter which in case of Hertzian contact is equal to 1.5 and  $x$  is the depth of penetration. An alternative model is being proposed and examined which implements an hysteresis of the ground in order to model particular soil kinds like wet sand or a stiff soil with a unified manner

$$F_g = \begin{cases} K \cdot x^n + B \cdot \dot{x} \cdot x^n, & \text{compr.} \\ \lambda \cdot K \cdot x^n + B \cdot \dot{x} \cdot x^n + F_{const}, & \text{rest.} \end{cases} \quad (21)$$

where

$$F_{const} = K \cdot x_{\max}^n \cdot [1 - \lambda] \quad \text{where } \lambda \geq 1 \quad (22)$$

and  $\lambda$  is an experimental coefficient which shows the irreversible and/or hysteric deformation of the ground during restitution, caused for example by a wet soil and  $x_{\max}$  the maximum depth during compression.

Friction can be accounted as in [15], depending on the soil characteristics (this value can be easily found in any textbook for soils) and the normal force during the interaction between the toe of the foot and the ground.

## 4. OPTIMAL GAITS

### 4.1. Extensive search

The extensive search scheme used in this work was set using the Matlab environment and has a two-layer structure. The inner layer involves the robot motion simulation. The equations of motion of each phase presented in Section 2.3 are solved using the ODE45 function and which set of them is solved each time is determined by the transition equations (1)-(4). The multipart controller function calculates during each flight phase the leg touchdown angles and actuator torques for the upcoming stance phase (rear, double or front). A simple PD-controller is used to position legs to the calculated desired touchdown angles. The robot motion simulation was set to be terminated when the robot had completed 65 strides, i.e. complete cycles considered from a reference limb, e.g. rear left, flight

phase till the next.

The outer layer involves definition of the initial conditions, the quadruped model physical parameters, the environment parameters and the desired motion parameters. This definition is programmed as a loop function to make the extensive search through a range of values of the parameters of interest feasible. In this work, parameters of interest include uncompressed leg length and stiffness, gravity and ground inclination, quadruped forward velocity, while Table 2 displays the parameter values that kept constant during the extensive search scheme.

Table 2. Constrained parameters during simulation.

Parameter	Value
Initial robot CM vertical position	0.35 m
Initial body pitch	0 rad
Initial body pitch rate	0.5 rad/ s
Initial vertical velocity	0 m/ s
Initial forward velocity	0.4 m /s
Body mass	9 kg
VLeg mass	0.62 kg
Prismatic joints viscous friction	10 Ns/ m
Hip joint distance	0.50 m
Body inertia	0.56 kgm <sup>2</sup>
Desired robot CM apex height	0.32 m

#### 4.2. MathWorks *fmincon*

The initial conditions, the quadruped model physical parameters, the environment parameters and the desired motion parameters influence directly the robot motion and its characteristics. We seek to find the optimum of them in order the robot to traverse a specific distance while consumes the least amount of energy, i.e. the actuators required torque. This is a constrained nonlinear multivariable problem and can be solved using MathWorks *fmincon* and an appropriate problem formalization.

The optimization vector is

$$\mathbf{x} = [\dot{x}_{cdes} \quad hdes \quad \dot{x}_0 \quad y_0 \quad \dot{\theta}_0 \quad k \quad l_0 \quad d] \quad (23)$$

where  $\dot{x}_{cdes}$  and  $hdes$  are the desired robot forward velocity and apex height respectively,  $\dot{x}_0$ ,  $y_0$  and  $\dot{\theta}_0$  are the initial forward velocity, vertical position and pitch rate respectively, while  $k$ ,  $l_0$  and  $d$  can be found in Table 1. The objective function is the square of the mean actuators required torque and its value is obtained running the robot motion simulation.

$$f(\mathbf{x}) = [\text{mean}(\text{torque})]^2 \quad (24)$$

The constraints definition involves inequalities of the optimization vector parameters, i.e.:

$$\begin{aligned} 0.1 &\leq \dot{x}_{cdes} \leq 5.0 \\ l_0 + 0.01 &\leq hdes \leq l_0 + 0.10 \\ 0 &\leq \dot{x}_0 \leq 1.0 \\ l_0 + 0.01 &\leq y_0 \leq l_0 + 0.10 \\ \dot{x}_{cdes} - \dot{x}_0 &\geq 0 \\ hdes - y_0 &\geq 0 \\ 0 &\leq \dot{\theta}_0 \leq 1.0 \\ 100 &\leq k \leq 20000 \\ 0.20 &\leq l_0 \leq 0.40 \\ 0.20 &\leq d \leq 0.30 \end{aligned} \quad (25)$$

and the initial vector  $\mathbf{x}_0$  has the following value:

$$\mathbf{x}_0 = [1.0 \ 0.30 \ 0.4 \ 0.35 \ 0.20 \ 6000 \ 0.25 \ 0.20] \quad (26)$$

#### 4.3. DE

The optimization method discussed in the previous section (that is the default algorithm underlying a call to the MATLAB *fmincon* solver) is a "local optimizer". In other words, its search is tailored at finding the closest valley to the initial guess. The complexity of the problem arising from the walking gaits optimization results in a rugged/discontinuous fitness landscape suitable for the deployment of a "global" optimization technique. In order to further explore the parameter space and the corresponding walking behaviours, we have thus also experimented with a heuristic global optimization method. In particular, we have used Differential Evolution (DE) [20]. The central idea behind DE is that the difference vector between two members of the population is added to a third member of the population, with which the performance is then compared. This scheme leads to excellent convergence properties, which was a necessary requirement for the optimization of the walking gaits due to the time spent in the inner loop optimization. The implementation used for the optimization is the MATLAB-script by Jim van Zandt [21], modified in order to deal with bounded variables.

Differential evolution has several good features, which makes it promising for complex searches. It is capable of searching in the whole design space (and not only in the basin of attraction the initial condition belongs to), does not require numerical differentiation, as it is a gradient free optimization method, it is easily parallelized in large CPU clusters using the island model and it is a well tested and highly regarded algorithm in the area of evolutionary computations.

The application of DE to our walking gaits problem revealed, though, several problems mainly connected to DE achieving very low fitness values with the solutions corresponding to unstable gaits or to non-physical solutions. Large portions of the search space apparently correspond to unphysical solutions, and we are now

identifying how to exclude such solutions from the search (possibly by incorporating more complex bounds). For this article, we reverted to the local search and we mainly present the results coming from that set of experiments.

## 5. RESULTS

### 5.1. Hildebrand Diagrams

We take for granted that the simulation environment can provide the ordinate values of the CM of the robot, their respective time values and their respective phase indicator.

At first, we compute the time moment in which the devolution from the transient to the steady state occurs so as to be able to discriminate between these two parts of the robot's locomotion. This is the time instance, for which, the pair of the local minimum value and the local maximum value of the robot's CM ordinate coordinate, which appear first, after that, (i.e., the transitional time), contains exactly these two CM ordinate values, that differ from each one of the following local minimums and local maximums, respectively, less than a user-defined tolerance. Here, you see that we need to compute the vector that holds the indexes that are respective to both the local maximum and minimum values of the CM ordinate (versus time). We do this by detecting the monotonous (increasing or decreasing) sub-arrays that form the one-dimensional array of CM ordinate values, and then, we save the index of each ordinate value that is located between a couple of these sub-arrays. These sub-arrays are alternated sequentially and that leads to an alternating finding of local maximums and minimums. We start with a find of a maximum value since we drop our robot in order to begin its movement.

Secondly, we compute four vectors that hold the lift-off (lo) and touchdown (td) time instances of both the hind (back) and the fore (front) feet. In order to build these four vectors ("lo\_hind" for the lo times of the hind feet, "td\_fore" for the td times of the fore feet, and, similarly, "td\_hind" and "lo\_fore") we check the succession of the phase indicators (integers in the range from one to four, 1 := double flight, 2 := back stance, 3 := double stance, 4 := fore stance) in a row-vector which is generated by the sets of differential equations which are successively integrated in order to produce the simulated movement. According to the result of this check (different every time, in general) we update the appropriate time vector with the time value that is respective to the last phase indicator which we inspected, before we detect a change in the values of the indicator vector, e.g., if at some part of this array the sequence of the indicators is [...] 1 1 1 1 2 2 2 2 [...] then we update the td\_hind vector with the time moment that is respective to the last "1" that appears.

To proceed, we calculate the three scalar quantities that form the gait diagrams. These quantities are the

duty factors (DF's) for both the hind and the fore feet and the phase relationship (PR) between the fore and hind ground contacts.

For the computation of the DF's (same procedure for both the hind and the fore feet) what we do is to compute every possible DF value that is respective to one of the distinguished gait cycles of the robot's movement and then we consider their mean value as the final outputted value. We adopt this procedure because we want to calculate the most typical value of each DF. The algorithm of computing one, of the many DF values, is fairly simple as it implements straight the definition schema [8]. For example, for the above-stated computation, we consider a pair of successive td time instances of a pair of feet and the unique lo event of the same pair of feet that is located between these two td events. At the end we calculate the ratio of the time interval that separates the first (smaller of the two) td value from the lo value to the time interval between the two td values. We apply this for every pair of adjacent td incidents of the current pair of feet (hind or fore) and then we take their mean value as stated above.

Subsequently, we compute the value of the PR between the footfalls of the hind and fore feet. To do this, we implement two different methods.

The first is the classical method [8], and, according to it, the value of the PR, of a gait, is equal to the ratio of the time interval between the td of the hind feet and the td of the fore feet (where hind footfall precedes fore footfall, since the stride here is defined as the robot movement between two successive footfalls of the hind feet) to the time interval between the two successive landings of the hind feet.

The second, is a variation of the classical method [22], and according to it, the PR value is equal to the ratio of the time interval between the td value of the fore feet and the td of the hind feet (here, the fore feet are used as reference in the definition of the gait cycle) to the time interval that separates the two consecutive touchdowns of the fore feet that are matched to the current gait.

To conclude, the PR computation is completed when we calculate every possible PR value, using both of the two pre-mentioned methods, and, at the end, we consider as our final value the mean value of all the realistic values that emerged.

Note that not all of the computed values are realistic, e.g., when the fore feet hit the ground before the hind feet in the "beginning" of two successive gaits, and, we use the "classic" computational method, we calculate a non-realistic value of the PR of the "first" gait, since the touchdown incident of the fore feet of that gait is located very close to the second touchdown of the hind feet of the same gait, in proportion to its stride duration (the time interval between two successive footfalls of the hind feet), i.e., it is a percentage of 0% to 25% which leads to a 75% to 100% value of PR. For a similar reason, the value of the PR, computed using the

alternate procedure, of the “first” gait of a couple of successive gaits where the hind feet touch the ground before the fore feet, in the beginning of that gait, is also non-realistic.

## 5.2. Results

The optimization procedure used to determine the optimum motion initial conditions, quadruped model physical parameters, environment parameters and the desired motion parameters related to energy efficiency. The optimization algorithms described in Section 4.2 and 4.3 were used and the results for Earth-like and Mars-like gravity are presented in Table 3.

Table 3. Optimization results.

	Earth	Mars
$\dot{x}_c des$	0.79	0.96
$hdes$	0.33	0.32
$\dot{x}_0$	0.79	0.52
$y_0$	0.34	0.37
$\dot{\theta}_0$	0.00	0.19
$k$	5631	6000
$l_0$	0.27	0.28
$d$	0.20	0.25

In order to plot the Hildebrand diagram of the gait that a quadruped robot uses in a given simulated locomotion, the algorithm presented in Section 5.1 was used. We can also use a gait graph, in which, a gait is represented by a dot with ordinate coordinate value equal to the PR, and abscissa coordinate value equal to the mean value of the hind and fore DF's.

Subsequently, we present two Hildebrand diagrams in Fig. 3 that are describing, respectively, the bounding gait and the pronking gait of a simulated quadruped robot motion. The values of the quantities that are associated to the simulation that lead to these diagrams are:  $m=9.22$  kg,  $l_0=0.3$  m,  $d=0.25$  m,  $k=4200$  N/ m,  $\dot{x}_0=0.4$  m/ s,  $y_0=0.35$  m,  $\dot{\theta}_0=0.50$  rad/ s,  $\dot{x}_c des=1.00$  m/ s,  $hdes=0.32$  m,  $g=9.81$  m/ s and  $0^\circ$  ground inclination.

For the inspection of the effects of the variation of a parameter in the gait selection we use a so-called “multiple” gait graph (a plane in which we depict the gait graphs of many simulated movements of the robot [8]) using the extensive search schema which is presented in the section 4.1, and, by plotting in the same plane different multiple gait graphs (each for a different planet or different ground inclination).

In Fig. 4, we vary the gravitational acceleration parameter for three different planets. The parameter values are the same as in Fig. 3 except for  $\dot{x}_0$  and  $y_0$  for Mars and Moon, in which are equal to  $0.5$  m/ s and

$0.32$  m, and,  $0.3$  m/ s and  $0.32$  m, respectively. Note that the horizontal line with ordinate value  $3\%$ , is defined to be the border that separates the pronking gaits (dots above that line) from the bounding gaits (dots below that line).

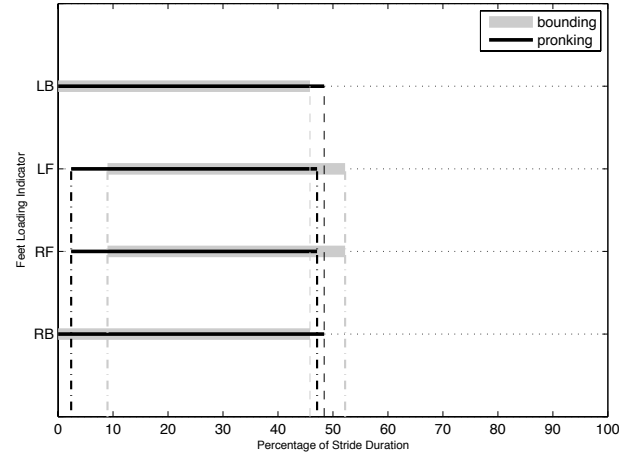


Figure 3. Bounding and pronking Hildebrand diagrams.

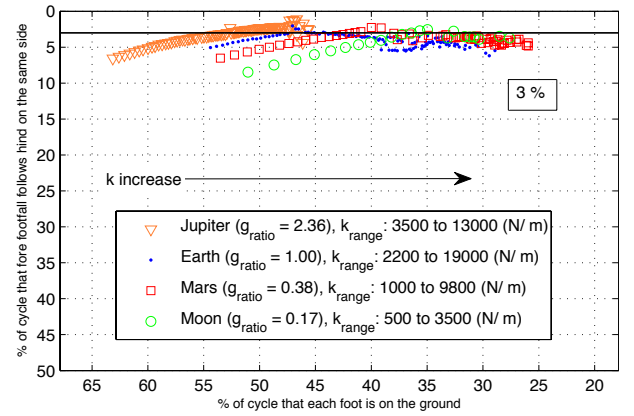


Figure 4. Gravity effect Hildebrand graph.

In Fig. 5, we vary  $k$  for planet Earth for three different ground inclination values. The rest of the required parameters are the same as in Fig. 3.

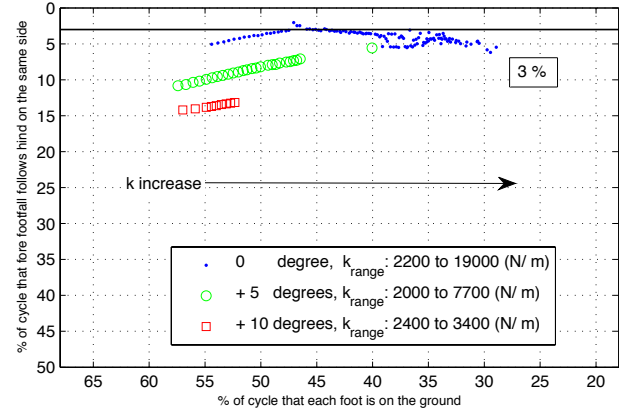


Figure 5. Ground inclination effect Hildebrand graph.

We also append a graph in which the alteration of

the  $r$  parameter, as it is defined in [23], is visualized while we vary  $k$  and  $g$ . Note that this figure is a version of the fig. 4 that contains only the gait graphs (dots), which lead to an  $r$  value that has not been observed until then. Again, the rest of the quantities are the same as in Fig. 3.

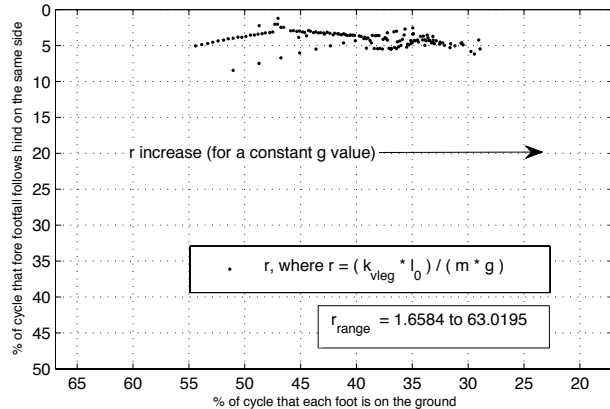


Figure 6. Compliance - gravity effect Hildebrand graph.

## 6. CONCLUSIONS

A procedure for implementing the computation of the Hildebrand diagrams has been proposed. Using this, and the extensive search philosophy, a set of results has been acquired, and, when analysing those, one observes that the increase of the value of the gravitational pull leads to the increase of the mean value of the DF's, the increase in the value of the ground inclination leads to the increase of the PR value and the increase of the leg's stiffness value leads to the decrease of the mean value of the DF's. Also, the range of the relative leg stiffness values has been presented, under the variation of leg stiffness and gravitational acceleration.

## ACKNOWLEDGEMENT

This work is performed under the Ariadna Call for Proposals: Space Gaits, contract number 4000105989/12/NL/KML.

## REFERENCES

1. Heverly, M. and Matthews, J. (2008). A Wheel-on-limb rover for lunar operation. *Proc. i-SAIRAS 2008*, Hollywood, USA.
2. Görner, M., Chilian, A. and Hirschmüller, H. (2010). Towards an Autonomous Walking Robot for Planetary Surfaces. *Proc. i-SAIRAS 2010*, Sapporo, Japan.
3. Chacin, M. and Yoshida, K. (2008). A Microgravity Emulation Testbed for Asteroid Exploration Robots. In *Proc. i-SAIRAS 2008*, Hollywood, USA.
4. Bartsch, S. et al. (2010). SpaceClimber: Development of a Six-Legged Climbing Robot for Space Exploration. *Proc. ISR/ROBOTIK 2010*, Germany.
5. Latta, M., Remy, C. D., Hutter, M., Höpflinger, M. and Siegwart, R. (2011). Towards Walking on Mars. In *Symposium of Advanced Space Technology in Robotics and Automation*, Noordwijk, Netherlands.
6. Muybridge, E., (1899), *Animals in Motion*, London: Chapman and Hall, Republished Dover Publications, New York, 1957.
7. Alexander, R. M., *Principles of Animal Locomotion*, Princeton, NJ: Princeton University Press, 2006.
8. Hildebrand, M., *The Quadrupedal Gaits of Vertebrates*, BioScience, Vol. 39, No. 11, Animals in Motion, Dec. 1989, pp. 766-775.
9. Cartmill, M., Lemelin, P., Schmitt, D., *Support polygons and symmetrical gaits in mammals*, Zoological Journal of Linnean Society, 136 (2002), pp. 401-420.
10. H. von Wachenfelt, Pinzke, S., Nilsson, C., Gait and force analysis of provoked pig gait on clean and fouled concrete surfaces, *Biosystems Engineering*, 104 (2009), pp. 534-544.
11. Raibert, M. *Legged Robots That Balance*, MIT Press, Cambridge, MA, 1986, pp. 92-95.
12. <http://nssdc.gsfc.nasa.gov/planetary/planetfact.html>
13. ESA, *MREP Mars Environmental Specification*, SRE-PAP/MREP/SFR-MES, Issue 1, Rev. 0, April 2010
14. Golembek, M. P. et al, "*The Martian Surface: Composition, Mineralogy, and Physical Properties*," ed. J.F. Bell III. Cambridge University Press 2008
15. Stronge, W. J., "*Impact Mechanics*," Cambridge University Press, 2000
16. Iagnemma, K., Kang, S., Shibly, H. and Dubowsky, S., "Online Terrain Parameter Estimation for Wheeled Mobile Robots With Application to Planetary Rovers," *IEEE Transactions on Robotics*, Vol. 20, No. 5, October 2004, pp. 921-927.
17. Caurin, G. and Tschichold-Gurman, N., "The development of a robot-terrain interaction system for walking machines," *IEEE ICRA 1994*, vol. 2, 1994.
18. Li, C, Zhang, T. and Goldman, D. I., "A Terradynamics of Legged Locomotion on Granular Media", *Science*, 339, pp. 1408-1412, 2013.
19. Gilardi, G. and Sharf I., "Literature Survey of Contact Dynamics Modelling", *Mechanism and Machine Theory* 37, pp. 1213-1239, 2002.
20. Storn, R. and Price, K., "Differential Evolution – A Simple and Efficient Heuristic for Global Optimization over Continuous Spaces," *Journal of Global Optimization* 11, pp. 341-359, 1997.
21. <http://www1.icsi.berkeley.edu/~storn/code.html#matl>
22. Renous, S., Herbin, M. and Gasc J.-P., *Contribution to the analysis of gaits: practical elements to complement the Hildebrand method*, Comptes Rendus Biologies, vol. 327, 2004, pp. 99-103.
23. Chatzakos, P., Papadopoulos, E. (2009). Bio-inspired Design of Electrically-Driven Bounding Quadrupeds via Parametric Analysis. *Mechanisms and Machine Theory*, 44(3), 559-579.